Dada *et al. Malar J* (2021) 20:414
https://doi.org/10.1186/s12936-021-03934-5

Malaria Journal

RESEARCH

Open Access

Comprehensive characterization of internal and cuticle surface microbiota of laboratory-reared F_1 *Anopheles albimanus* originating from different sites

Nsa Dada[1,4,5*], Ana Cristina Benedict[2], Francisco López[2], Juan C. Lol[2], Mili Sheth[3], Nicole Dzuris[1], Norma Padilla[2] and Audrey Lenhart[1]

Abstract

Background: Research on mosquito-microbe interactions may lead to new tools for mosquito and mosquito-borne disease control. To date, such research has largely utilized laboratory-reared mosquitoes that typically lack the microbial diversity of wild populations. A logical progression in this area involves working under controlled settings using field-collected mosquitoes or, in most cases, their progeny. Thus, an understanding of how laboratory colonization affects the assemblage of mosquito microbiota would aid in advancing mosquito microbiome studies and their applications beyond laboratory settings.

Methods: Using high throughput 16S rRNA amplicon sequencing, the internal and cuticle surface microbiota of F_1 progeny of wild-caught adult *Anopheles albimanus* from four locations in Guatemala were characterized. A total of 132 late instar larvae and 135 2–5 day-old, non-blood-fed virgin adult females that were reared under identical laboratory conditions, were pooled (3 individuals/pool) and analysed.

Results: Results showed location-associated heterogeneity in both F_1 larval internal ($p=0.001$; pseudo-$F=9.53$) and cuticle surface ($p=0.001$; pseudo-$F=8.51$) microbiota, and only F_1 adult cuticle surface ($p=0.001$; pseudo-$F=4.5$) microbiota, with a more homogenous adult internal microbiota ($p=0.12$; pseudo-$F=1.6$) across collection sites. Overall, ASVs assigned to *Leucobacter, Thorsellia, Chryseobacterium* and uncharacterized *Enterobacteriaceae,* dominated F_1 larval internal microbiota, while *Acidovorax, Paucibacter,* and uncharacterized *Comamonadaceae,* dominated the larval cuticle surface. F_1 adults comprised a less diverse microbiota compared to larvae, with ASVs assigned to the genus *Asaia* dominating both internal and cuticle surface microbiota, and constituting at least 70% of taxa in each microbial niche.

Conclusions: These results suggest that location-specific heterogeneity in filed mosquito microbiota can be transferred to F_1 progeny under normal laboratory conditions, but this may not last beyond the F_1 larval stage without adjustments to maintain field-derived microbiota. These findings provide the first comprehensive characterization of laboratory-colonized F_1 *An. albimanus* progeny from field-derived mothers. This provides a background for studying

*Correspondence: nsadada@yahoo.com
[1] Entomology Branch, Division of Parasitic Diseases and Malaria, Center for Global Health, United States Centers for Diseases Control and Prevention, Atlanta, GA, USA
Full list of author information is available at the end of the article

how parentage and environmental conditions differentially or concomitantly affect mosquito microbiome composition, and how this can be exploited in advancing mosquito microbiome studies and their applications beyond laboratory settings.

Keywords: Mosquito microbiota, *Anopheles albimanus*, Laboratory colonization, Mosquito microbiome, Next generation sequencing, 16S rRNA gene amplicon sequencing

Background

Mosquitoes contain microbes that inhabit various tissues, such as the alimentary canal, reproductive organs, and cuticle surface [1]. These microbes are thought to be principally obtained from the mosquito habitat during larval development, and from food sources at the adult stage [1]. In addition to acquisition from larval habitats and/or adult food sources, transovarial bacterial transmission from adult females to their eggs, and transstadial transmission across different immature stages, and into the adult stage, have been demonstrated [2, 3]. As a key component of the mosquito microbiota, environmentally-acquired microbes have been shown to affect mosquito life history traits such as the rate of pupation and adult body size [4]. The mosquito microbiota has also been shown to affect the following aspects of mosquito biology: immunity to human pathogens [5], reproduction [6], insecticide resistance [7, 8], and ultimately vector competence—the mosquito's ability to acquire, maintain and transmit pathogens [5]. These effects of the microbiota on mosquito biology are being leveraged to develop novel approaches for mosquito-borne disease control [9].

The use of next generation molecular biology tools has resulted in extensive characterization of mosquito microbiota, with the initial focus on bacterial and archaeal components now expanding to eukaryotic microbes [10, 11] and viruses [12, 13]. These advances in mosquito microbiota research have led to field applications of mosquito symbionts for mosquito control. For *Aedes aegypti*, the principal vector of dengue, Zika, Chikungunya and yellow fever viruses, mosquito-derived symbionts are now being used to suppress mosquito populations [14] and also being considered to control the spread of pathogens [15]. However, studies exploring mosquito symbionts for malaria control have largely remained at the laboratory stage [16, 17]. Similarly, the microbiota of mosquito vectors in some geographical regions are well characterized and studied compared to those from other regions. In malaria vectors for example, studies on the microbiota have largely focused on sub-Saharan African species—in particular, *Anopheles gambiae*—and to a lesser extent on those from Southeast Asia [18]. In contrast, the microbiota of Latin American malaria vectors have only recently been comprehensively characterized [7, 8, 19–21], with these studies describing associations between *Anopheles albimanus* microbiota and insecticide resistance [7, 8], and the factors that shape the composition of *An. albimanus*, *Anopheles darlingi*, *Anopheles nunetzovari*, *Anopheles rangeli,* and *Anopheles triannulatus* microbiota [19–21].

To exploit the mosquito microbiota for malaria and malaria vector control, research must successfully advance from laboratory to field settings, a transition which can be fraught with challenges. For example, some malaria vectors such as *An. darlingi, Anopheles vestitipennis,* and *An. gambiae* can breed in sites that are small, temporary and difficult to find and/or access [22–26], making it hard to obtain sufficient immature field mosquitoes for experiments. Where larval habitats are plentiful and easy to find and/or access, the subsequent rearing of field-collected mosquitoes to obtain uniform characteristics can pose additional challenges [27, 28].

Additionally, some malaria vectors belong to species complexes whose members are morphologically indistinguishable [29–32], constituting another layer of complexity that needs to be considered in elucidating mosquito-microbe interactions in malaria vectors.

These challenges, which are common to research on mosquito ecology and control, are often not reported or discussed in mosquito microbiome studies. Several failed attempts at collecting and rearing sufficient immature mosquitoes from the field for our previous study on the role of mosquito microbiota in insecticide resistance resulted in ultimately using either wild-caught adults [7] or F_1 progeny derived from field-collected adult mosquitoes [8, 33]. While field-caught adult mosquitoes or their F_1 progeny may offer insights into mosquito-microbe interactions in field scenarios, obtaining adult field-collected mosquitoes with uniform and/or controlled physiological characteristics is usually not feasible. Although location-associated heterogeneity in microbiota of field-collected mosquitoes has been previously described [34, 35], there is limited information on the fate of field-acquired microbiota after laboratory colonization of field-collected mosquitoes. So far, it has been observed that upon eclosion, newly-emerged laboratory-reared adult mosquitoes show a reduction in bacterial diversity in contrast to earlier developmental stages [36]. In addition, a recent study on the fate of field-acquired microbiota in laboratory-colonized *An. gambiae* sensu lato (*s.l.*)

showed a reduction in bacterial diversity of the F_5 progeny (the first point of measurement) that were reared in dechlorinated tap water in contrast to F_0 [37]. Another study of *Ae. aegypti* from different locations showed no associations between location and microbiota composition after several generations of laboratory colonization [38]. At what point the microbiota of laboratory-colonized mosquitoes become homogenous and whether the microbiota of F_1 laboratory progeny represent their parental origin—and thus could be used for symbiont-based translational studies—remains largely undescribed.

Here, a comprehensive characterization of the microbiota of laboratory-reared F_1 progeny from field-caught adult *An. albimanus* is presented. These represent unanticipated findings from a larger study that was aimed at characterizing the effects of insecticide exposure and resistance on *An. albimanus* microbiota [8]. Little or no immediate loss of location-associated heterogeneity in microbial composition upon initial laboratory colonization was expected, based on evidence of this type of heterogeneity in field-derived populations [34, 35], or at least, consistency in microbiota composition across the F_1 progeny as a function of their collection sites or rearing conditions. However, the resulting data showed location-associated heterogeneity in both F_1 larval internal and cuticle surface microbiota, and only F_1 adult cuticle surface microbiota, with a more homogenous adult internal microbiota. These findings lay the foundations for studying how parentage and environmental conditions differentially or concomitantly affect mosquito microbiome composition, and how this can be exploited in advancing mosquito microbiome studies and their applications beyond laboratory settings.

Methods

The findings presented here extend those of a larger study [8]. Thus, the mosquito collection, processing and sequencing procedures have previously been described in detail [8].

Mosquito collections and laboratory generation of F_1 progeny

Gravid and/or blood-fed adult female *An. albimanus* were sampled across four field sites in the villages of Las Cruces and El Terrero, in La Gomera, department of Escuintla, Guatemala (Fig. 1). Field-collected mosquitoes from each location were held in separate paper cups, sustained on 10% sucrose solution, and transported to the insectary at Universidad del Valle de Guatemala in Guatemala City for species identification, oviposition and subsequent rearing of F_1 progeny. Mosquitoes that were morphologically identified as *An. albimanus* following identification keys [39] (approximately 300 in total that had a white terminal palpal segment, white third and fourth hind tarsomeres, and basal dark band on their fifth hind tarsomere) were subjected to oviposition, and a subsample of the resulting F_1 progeny was used for molecular verification of species identity as described below. A modified oviposition procedure [40] was employed, wherein no more than 70 gravid females

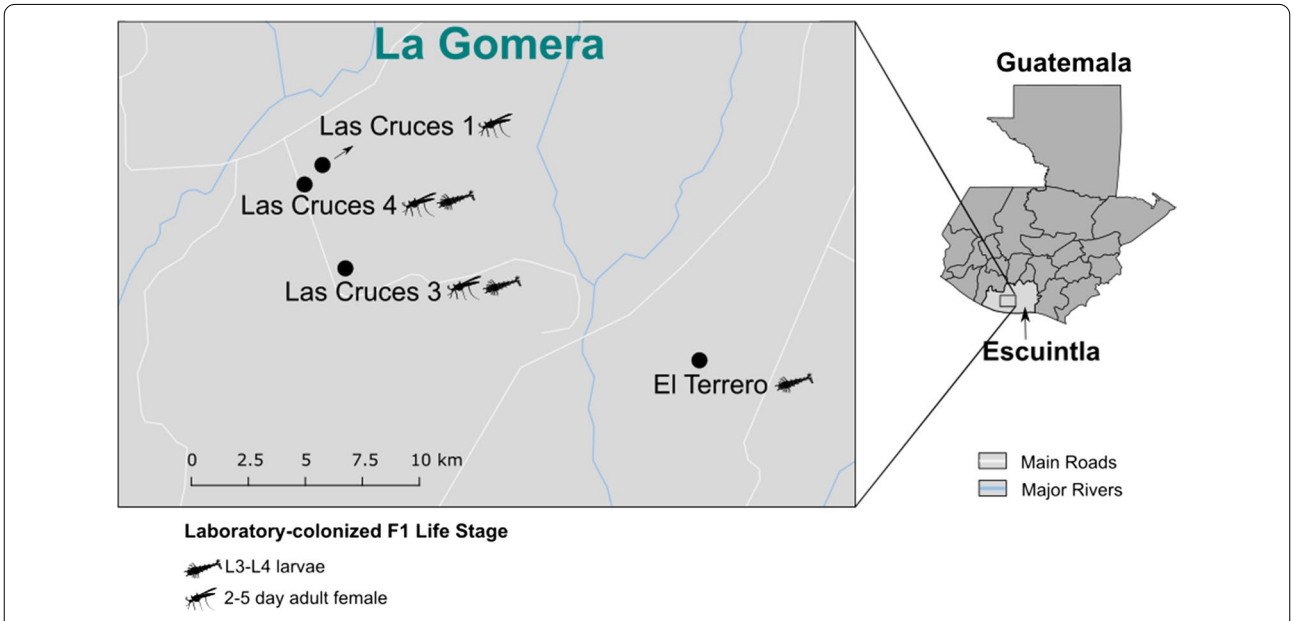

Fig. 1 Map showing the maternal origins of F_1 *Anopheles albimanus*. F_1 laboratory-colonized mosquitoes were derived from gravid and/or blood fed females collected from each location. Mosquito icons show the maternal origin of the F_1 life stages studied

from the same location were placed in quart size paper ice cream containers with distilled water to a depth of at least 2 cm. The containers were covered with fine mesh fabric that were secured with rubber bands prior to the introduction of gravid field-caught adult *An. albimanus*. The mesh was topped with cotton balls soaked in 10% sucrose to sustain the mosquitoes, and subsequently covered with a thick piece of black plastic bag to keep the containers dark and trap in moisture. The oviposition chambers were held under the following insectary conditions; 27 ± 2 °C, 80 ± 10% relative humidity, and 12-h light–dark cycle. After at least 48 h, the adult females were removed and discarded as they were not needed for the original study. The F_1 eggs were collected, pooled by location and reared separately under identical ambient conditions (as described above) and the following larval feeding regimen. Eggs were washed into 18 × 14 × 3 inch plastic larval trays (approximately 200 eggs per tray) containing distilled water to a depth of at least 2 cm, and 3–4 drops of 10% yeast solution. Hatched larvae were sustained on finely ground Koi fish food (Foster & Smith, Inc. Rhinelander, WI) until pupation. At the third to fourth larval instar stage (L3-L4), half of the larvae were separated and used for bioassays in the original study and subsequently processed for microbiota characterization (n = 132). Using a stereo microscope, female pupae from the remaining mosquitoes were separated into 8 oz. paper ice cream cups and placed into cardboard cages for adult eclosion. The resulting F_1 adult virgin female mosquitoes were sustained on 10% sucrose solution until they were 2–5 days old and also used for bioassays in the parent study. These were subsequently processed for microbiota characterization (n = 135). Post bioassays, larval and adult samples were preserved in RNALater® solution (Applied Biosystems, Foster City, CA), shipped on dry ice to the US Centers for Disease Control and Prevention (CDC) in Atlanta, USA, and stored at -80 °C until further processing. Samples originating from different locations were handled, stored and processed separately.

Genomic DNA extraction from mosquito legs, whole mosquito samples, and mosquito cuticle surfaces

Stored mosquito samples were thawed overnight at 4 °C, and the thawed RNALater® solution was discarded. This was followed by a rinse with nuclease-free water to remove any residual RNALater®. Legs from a subsample of individual F_1 adults were removed using sterile forceps and placed in individual sterile1.5 mL Eppendorf tubes containing 75 µL Extracta DNA Prep solution (Quantabio, Beverly, MA) for DNA extraction following manufacturer's instructions. Both larvae and adult (with and without legs removed) F_1 samples were pooled for whole body and cuticle surface DNA extractions. Each pool comprised 3 individuals, resulting in 44 pools of larvae and 45 pools of adults. Table 1 shows the number of pools (replicates) processed per life stage and collection site. To obtain cuticle surface samples, each pool was submerged in 500 µL of nuclease free water and washed vigorously by agitating with a vortex mixer for at least 15 s. The resulting wash water was transferred to new sterile tubes for DNA extraction, acknowledging that some microbes may have been lost via rinsing off the preservative (RNALater® solution) prior to this step. A comprehensive (comparable or more than the internal community) microbial community was nonetheless recovered from the cuticle surface samples. The washed sample pools were further surface sterilized using two vigorous washes; first in 70% ethanol, then nuclease free water, each with at least 15 s agitation on a vortex mixer. This was followed by one gentle rinse with nuclease free water. Genomic DNA from the surface-sterilized samples and wash water (subsequently referred to as internal and cuticle surface, respectively) was isolated using the TissueLyser II and DNeasy Blood and Tissue Kit (QIAGEN, Hilden, Germany) as follows: in individual 2 mL sterile tubes, 180 µL of buffer ATL (QIAGEN) and 5 mm diameter stainless steel beads (QIAGEN) were added to each sample pool. With the following settings: 30 Hz/s for 8 and 15 min for internal and cuticle surface samples respectively, samples were homogenized using the TissueLyser (QIAGEN) fitted with two sets of 96-well adapter plates that held the tubes. The plates were rotated every minute during homogenization, and afterwards, samples were transferred into new sterile 1.5 mL Eppendorf tubes for the remaining part of the DNA extraction process. 20 µL of Proteinase K (QIAGEN) was added to each homogenized sample and incubated overnight at 56 °C, after which 200 µL of buffer AL (QIAGEN) was added and incubated for a further 2 h at the same temperature. The remaining steps were performed according to QIAGEN's spin-column protocol for purification of DNA from animal tissues, and the purified DNA was eluted in 70 µL of buffer AE (QIAGEN). Two sets of two

Table 1 Number of laboratory colonized F_1 *An. albimanus* processed, per life stage and collection site

Collection site	Number of mosquitoes (number of pools)	
	L3–L4 larvae	Adult ♀s
El Terrero	45 (15)	–
Las Cruces 1	–	27 (9)
Las Cruces 3	42 (14)	45 (15)
Las Cruces 4	45 (15)	63 (21)

blank controls (without samples) were processed alongside the internal and cuticle surface samples, and all steps, along with those described below, were performed under sterile conditions. The purified genomic DNA from samples and blank controls were stored at -80 °C until further processing.

Molecular species confirmation of *An. albimanus* and 16S rRNA amplicon sequencing

DNA samples from mosquito legs were used as templates to amplify the second internal transcribed spacer region (ITS2) of the mosquito ribosomal DNA in order to verify morphological identification of *An. albimanus*. This was achieved by conventional PCR using the universal ITS2 primers (ITS2 A: TGTGAACTGCAGGAC ACAT and ITS2 B: TATGCTTAAATTCAGGGGGT) for distinguishing members of *Anopheles* complexes [41], and known *An. albimanus* DNA as positive control. With a final reaction volume of 25 µL, each PCR comprised ≥ 100 ng/µL DNA template, 15 µM of each primer, 12.5 µL of 2X AccuStart II PCR SuperMix (Quantabio, Beverly, MA), and PCR grade water to final volume. With the following conditions, initial denaturation at 94 °C for 4 min, then 35 cycles of 94 °C for 30 s, 53 °C for 40 s, and 72 °C for 30 s, followed by a final extension for 10 min at 72 °C, the reactions were performed using a T100™ Thermal Cycler (Bio-Rad, USA). Using EtBr-stained agarose gel electrophoresis, the amplified products which showed bands of the same size as that of the positive control ~ 500 bp, confirmed all samples as *An. albimanus* [42].

DNA from internal and cuticle surface samples, along with those from blank controls, were used as templates to amplify the universal bacterial and archaeal 16S rRNA gene. This was also achieved by conventional PCR using universal primers targeting the v3-v4 region of the 16S rRNA gene (341F: **TCGTCGGCAGCGTCAGATGTG TATAAGAGACAG**CCTACGGGNGGCWGCAG, and 805R: **GTCTCGTGGGCTCGGAGATGTGTATAA GAGACAG**GACTACHVGGGTATCTAATCC), each with Illumina® (San Diego, CA USA) adapters (bold typeface). With a final reaction volume of 25 µL, each PCR comprised; ≥ 20 ng/µL DNA template, 5 µM of each primer, 10 µL of 2 × KAPA HiFi HotStart PCR mix (Roche, Switzerland), and PCR grade water to final volume. Three negative controls with PCR grade water substituted for DNA template, were processed along with the samples. The reactions were performed using the T100™ Thermal Cycler (Bio-Rad, USA) under the following conditions; initial denaturation at 95 °C for 3 min, then 25 cycles of 95 °C, 55 °C, and 72 °C for 30 s each, followed by a final extension for 5 min at 72 °C. The amplification products, sized ~ 460 bp, were verified by electrophoreses as described above and quantified using a NanoDrop™ spectrophotometer (Thermo Fisher Scientific, Waltham, MA). Amplicons, including PCR products from blanks and negative controls, which yielded no bands following electrophoresis, were purified using Agencourt AMPure XP beads (Beckman Coulter Inc., Indianapolis, IN, USA) at 0.7X (internal) or 0.875X (cuticle surface) sample volume, and eluted in 40 µL of 10 mM Tris buffer (pH 8.5).

All purified products, including those of blanks and negative controls, were used as templates for sequencing library preparation. This was accomplished via index PCR using the Nextera XT Index kit v2 sets, A, B and D (Illumina, San Diego, CA). With a final reaction volume of 50 µL, each index PCR comprised; 25 µL NEBNext High-Fidelity 2X PCR master mix (New England Biolabs Inc., Ipswich, MA), 5 µL of each index primer, 10 µL of purified PCR products (0–20 ng/µL) as template, and PCR grade water to final volume. The PCRs were performed under the following reaction conditions; 98 °C for 30 s, then 8 cycles of 98 °C for 10 s, 55 °C and 65 °C for 30 s each, and a final extension at 65 °C for 5 min, and resulting libraries were also cleaned using Agencourt AMPure XP beads (Beckman Coulter Inc., Indianapolis, IN, USA) at 1.2X sample volume and eluted in 25 µL of 10 mM Tris buffer (pH 8.5). The libraries were subsequently analysed for size and concentration, normalized to 2 nM, pooled and denatured following Illumina guidelines for loading onto flowcells. Sequencing was performed on an Illumina HiSeq 2500 machine, using 2 × 250 cycle paired-end sequencing kits.

Preprocessing of sequencing reads

Sequencing outputs were demultiplexed and converted to the fastq format for downstream analysis using the bcl2fastq (v2.19) conversion software (Illumina®). A total of 115,250,077 demultiplexed paired-end sequencing reads, with a maximum length of 250 bp were initially imported into the 'quantitative insights into microbial ecology' pipeline, QIIME2 v.2017.7.0 [43], and further sequencing read processing and analysis were performed in v.2018.2.0 of the pipeline. Using the DADA2 plugin in QIIME 2 [44], the denoise-paired command with the following options; trunc_len_f: 244, trunc_len_r: 244, and n_reads_learn: 500,000, was used to correct errors, remove chimeras and merge paired-end reads. The resulting amplicon sequence variants (ASVs; n = 30,956,883) were further filtered to remove potentially extraneous ASVs (those with < 100 counts) and ASVs that were associated with blanks and negative controls. This last filtering step resulted in 17,225,776 ASVs, ranging from 3,277 to 223,222 per sample (mean 96,774), that were used for downstream comparison of bacterial composition and

taxonomic analysis. Additional file 3. shows sequencing reads and ASV summary statistics.

Diversity indices

Analysis of microbial diversity within (alpha diversity) and between (beta diversity) samples were performed in QIIME2 using the Shannon diversity index and Bray–Curtis dissimilarity index, respectively. The Shannon diversity indices were calculated using rarefied ASVs counts per sample, in which ASVs per sample were selected randomly without replacement at an even depth (Additional file 4) for ten iterations. The resulting average Shannon indices are presented and were compared between samples using pairwise Kruskal–Wallis tests with Benjamini–Hochberg false discovery rate (FDR) corrections for multiple comparisons.

The Bray–Curtis dissimilarity indices were computed with or without rarefaction, and resulting indices were compared between samples using pairwise PERMANOVA tests (999 permutations) with FDR corrections. There were no discernable differences between results of rarefied and non-rarefied data. Thus, results of Bray–Curtis dissimilarity indices using non-rarefied data were visualized by Principal Co-ordinates Analysis (PCoA) plots in R [45] using the phyloseq R package [46]. Significance for both pair-wise analyses was set to $q < 0.05$ (i.e. post FDR p-value corrections).

Taxonomic analysis and differentially abundant microbial taxa

Taxonomic analysis of ASVs was performed using QIIME2's pre-trained Naïve Bayes classifier [47] and q2-feature-classifier plugin [48]. Prior to analysis, the classifier was trained on the QIIME-compatible 16S SILVA reference (99% identity) database v.128 [49], and using the extract-reads command of the q2-feature-classifier plugin, the reference sequences were trimmed to the v3-v4 region (425 bp) of the 16S rRNA gene. The frequency of annotated ASVs across samples were subsequently visualized using the qiime feature-table heatmap plugin based on Bray–Curtis distances with the plugin's default clustering method. Only annotated ASVs with counts ≥ 2000 (larvae) or ≥ 1000 (adults) were included in the heatmaps.

Differentially abundant microbial taxa across locations were identified using QIIME2's analysis of composition of microbiomes (ANCOM) [50] plugin. The cut-off for differential abundance was set to an effect size of log $F \geq 20$ and $W \geq 20$, i.e. a taxon was differentially abundant across collection sites if the ratio of its abundance to those of at least 20 other taxa (25% of all included taxa) differed significantly across sites.

Prior to each analysis, ASV frequency data was normalized by $\log_{10}$ transformation following the addition of pseudocounts of 1. To ensure that filtering of low frequency reads did not compromise the findings, all downstream analyses were also performed with these reads included, and results (Additional file 5) were consistent with those of the clean/filtered dataset. Results of the clean dataset are subsequently discussed. The outputs of data analyses were aesthetically formatted using Inkscape [51].

Results

Using high throughput deep sequencing of the universal bacterial and archaeal 16S rRNA gene, we characterized the microbiota of the internal and cuticle surface microbial niches of laboratory reared *An. albimanus* F_1 larvae ($n = 132$) and adult ($n = 135$) progeny from mothers that were collected from four locations in south central Guatemala (Fig. 1). Mosquitoes were processed as pools (3 individuals per pool), resulting in a total of 44 larval and 45 adult pools. F_1 larvae were from El Tererro, Las Cruces 3 and Las Cruces 4, while F_1 adults were from Las Cruces 1, Las Cruces 3 and Las Cruces 4 (Table 1). Following quality control of the resulting sequencing reads, amplicon sequence variants (ASVs) were identified and used in downstream analysis. Since adult mosquito microbiota is distinct from that of immature stages [52, 53], ASVs from larvae and adults were analysed separately, as were ASVs from each microbial niche (internal or cuticle surface).

Internal and cuticle surface microbiota of laboratory colonized F1 *An. albimanus* larvae differed by location

Non-pairwise Bray–Curtis distance comparison showed significant differences in internal ($p = 0.001$) and cuticle surface ($p = 0.001$) microbiota between F_1 larvae from different collection sites. Thus, irrespective of microbial niche, the microbial community structure (composition and relative abundance of ASVs) of F_1 laboratory-colonized larvae differed by collection location. Pairwise PERMANOVA comparison of Bray–Curtis distances further showed significant differences in microbial community structure in larval internal ($q < 0.01$) and cuticle surface microbiota ($q < 0.01$) between every pair of collection site (Table 2). This location-driven heterogeneity in microbial community structure was further demonstrated by principal coordinate analysis (PCoA), where F_1 larval internal and cuticle surface microbiota clustered distinctly by collection site (Fig. 2).

Non-pairwise Shannon diversity comparisons showed significant differences in internal ($p = 0.009$) but not cuticle surface ($p = 0.09$) microbiota of F_1 laboratory-colonized larvae from different collection sites, indicating that there was inter-sample variation in the diversity of

Table 2 Pairwise beta and alpha diversity comparisons of laboratory colonized F_1 *An. albimanus* microbiota from different collection sites. Bray-Curtis diversity comparison showed significant differences in larval internal and cuticle surface microbiota between collection sites. In contrast, only adult cuticle surface but not internal microbiota were significantly different across collection sites. These comparisons were conducted using PERMANOVA (999 permutations) tests, with Benjamini-Hochberg FDR correction (q-value). Significance was determined at $q < 0.05$. n = No. of pools processed, and each pool comprised three individual mosquitoes.

	Group 1	Group 2	Internal			Cuticle surface		
			pseudo-F	p-value	q-value	pseudo-F	p-value	q-value
Adults	LasCruces1 (n = 9)	LasCruces3 (n = 15)	2.21	0.088	0.161	**5.80**	**0.001**	**0.003**
	LasCruces1 (n = 9)	LasCruces4 (n = 21)	1.92	0.107	0.161	**4.97**	**0.004**	**0.005**
	LasCruces3 (n = 15)	LasCruces4 (n = 21)	0.85	0.443	0.443	**3.07**	**0.005**	**0.005**
Larvae	ElTerrero[a] (n = 15)	LasCruces3 (n = 14)	**9.81**	**0.001**	**0.001**	**4.48**	**0.001**	**0.001**
	ElTerrero[a] (n = 15)	LasCruces4 (n = 15)	**7.98**	**0.001**	**0.001**	**11.43**	**0.001**	**0.001**
	LasCruces3 (n = 14)	LasCruces4 (n = 15)	**10.88**	**0.001**	**0.001**	**11.37**	**0.001**	**0.001**

[a] Two pools were exlcuded from the analysis of cuticle surface microbiota following rarefaction

internal but not cuticle surface microbiota of larvae when all collection sites were taken into consideration. A pairwise Kruskal–Wallis comparison of Shannon diversity indices showed that the inter-sample variation in diversity of larval internal microbiota held true when every pair of collection sites was considered except between Las Cruces 3 and 4 (Table 3 and Additional file 1). Larvae originating from Las Cruces 3 had the highest internal microbiota diversity, followed by Las Cruces 4 and El Terrero (Additional file 1).

Cuticle surface, but not internal, microbiota of laboratory colonized F1 adult *An. albimanus* differed by location

Non-pairwise Bray–Curtis diversity comparisons showed significant differences in cuticle surface ($p = 0.001$), but not internal microbiota ($p = 0.12$) between adult F_1 mosquitoes from different collection sites, suggesting a loss of location-driven heterogeneity in microbial community structure in internal but not cuticle surface microbial niche of laboratory-colonized F_1 adults. Pairwise PERMANOVA comparisons of Bray–Curtis distances also showed significant differences in microbial community structure of F_1 adult cuticle surface microbiota ($q < 0.01$) between every pair of collection sites (Table 2). These results were corroborated by PCoA, which showed that F_1 adult cuticle surface microbiota, but not internal microbiota, clustered distinctly by collection site (Fig. 2).

Non-pairwise Shannon diversity comparisons showed no differences in the internal ($p = 0.42$) or cuticle surface ($p = 0.4$) microbiota of F_1 adults from different collection sites, indicating that there was little or no inter-sample variation in diversity of F_1 adult microbiota when all collection sites were taken into consideration. Pairwise Kruskal–Wallis comparisons of Shannon diversity indices also detected no inter-sample variation in diversity of F_1 adult cuticle surface or internal microbiota when every pair of collection site was considered (Table 3 and Additional file 1).

Laboratory-colonized F1 *An. albimanus* larvae comprised a rich and diverse microbiota that differed by location

Overall, ASVs from larval internal microbiota were assigned to 180 bacterial taxa, and cuticle surface microbiota to 194 bacterial taxa (Additional file 2.). A majority of these taxa across all locations (ranging from 118 to 139 taxa) were shared between the internal and cuticle surface microbiota (Fig. 3a), as well as across collection sites ($n = 110$ for cuticle surface and $n = 117$ for internal microbiota) (Fig. 3b). While a majority of the identified microbial taxa were shared between both microbial niches, their abundance was generally higher in internal (Fig. 4a) compared to cuticle surface (Fig. 4b) microbiota. Although a majority of identified microbial taxa in both internal and cuticle surface microbiota were shared across all locations, their abundance differed by location (Fig. 4a, b and 5).

In general, larval internal microbiota was dominated by ASVs identifed as an uncharacterized *Enterobacteriaceae, Leucobacter, Thorsellia,* and *Chryseobacterium* (Fig. 4a), together making up over 50% of ASVs (Additional file 2). In contrast, *Acidovorax,* unchracterized *Comamonadaceae,* and *Paucibacter* (Fig. 4b) made up over 50% of ASVs detected on the larval cuticle surface (Additional file 2).

A few predominant bacterial taxa were present in the larval internal microbial niche across all three collection sites: unclassified *Enterobacteriaceae, Thorsellia, Rhizobium, Xantobacter, Acidovorax* and *Pirellula* (Fig. 4a.), with remaining taxa showing different patterns of abundance between collection sites (Fig. 5 and Additional file 2). For example, ASVs assigned to the genus *Azoracus* were predominant in larvae from El Terrero, while

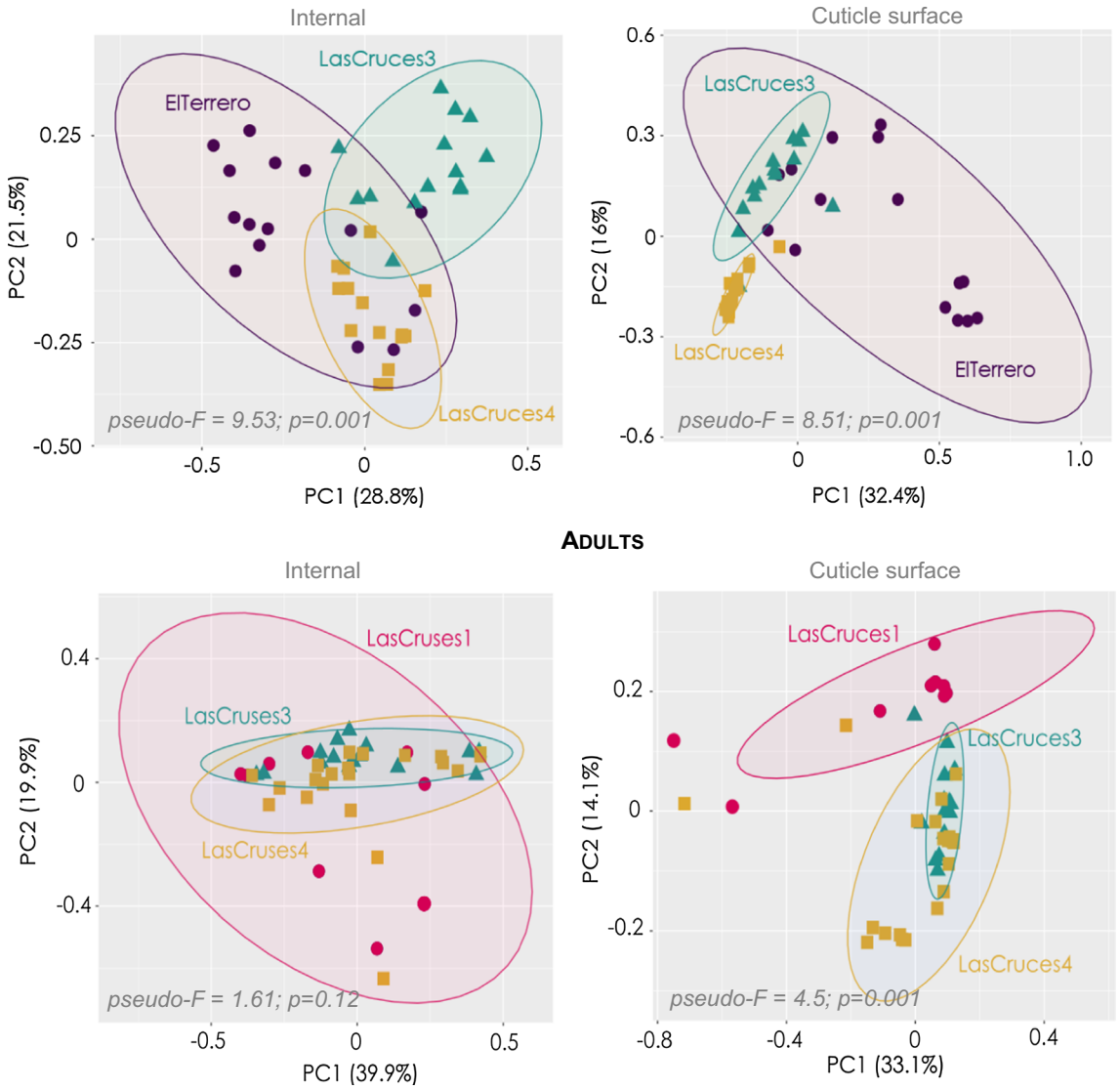

Fig. 2 Principal coordinate analysis (PCoA) ordinations of internal and cuticle surface microbiota from F_1 laboratory-colonized *An. albimanus*. The PCoA plots are based on Bray–Curtis distances between the microbiota of mosquitoes with differing collection sites. Each point on the plot represents the microbial composition of a pool of three individuals, and mosquito pools are color-coded by their origin. For larvae, the first two principal component (PC) axes captured 50% (internal) and 48% (cuticle surface) of the variance in the data, with both internal and cuticle surface microbiota clustering distinctly by collection site. For adults, the first two PC axes captured 59% (internal) and 47% (cuticle surface) of the variance in the data, with cuticle surface but not internal microbiota clustering distinctly by collection site. PERMANOVA statistics are presented at the bottom of each plot

Singulisphaera, Paucibacter, Ancylobacter, Gemmobacter, and *Rayranella* were predominant in those from Las Cruces 3. Predominant in larvae from Las Cruces 3 and Las Cruces 4 were *Azospirillum, Bosea* and *Microbacterium*; and in those from El Terrero and Las Cruces 3 were *Terrimicrobium* and *Legionella* (Fig. 5). Although outside of the cut off limit set for differential abundance, ASVs assigned to the bacterial genera *Leucobacter* were predominant in the internal microbiota of larvae from Las Cruces 4 and El Terrero, but predominant in only three of the 14 sample pools from Las Cruces 3 (Fig. 4a). Similarly, *Chryseobacterium* was predominant in Las Cruces 4 and 3, but only predominant in six of the 16 pools of larvae from El Terrero. Bacterial taxa that were unique to each location comprised < 8% of all taxa in larval internal microbiota (Additional file 3b), and were

Table 3 Pairwise alpha diversity comparisons of laboratory colonized F_1 *An. albimanus* microbiota from different collection sites. Shannon diversity comparison showed significant differences in larval internal but not cuticle surface microbiota between collection sites (two of the three pairs). In contrast, there was no significant difference in adult internal or cuticle surface microbiota between collection sites. These comparisons were conducted using Kruskal-Wallis tests, with Benjamini-Hochberg FDR correction (q-value). Significance was determined at $q < 0.05$. n = No. of pools processed, and each pool comprised three individual mosquitoes.

	Group 1	Group 2	Internal			Cuticle surface		
			H	p-value	q-value	H	p-value	q-value
Adults	LasCruces1 (n = 9)	LasCruces3 (n = 15)	0.00	0.98	0.98	1.09	0.30	0.41
	LasCruces1 (n = 9)	LasCruces4 (n = 21)	0.49	0.48	0.72	1.23	0.27	0.41
	LasCruces3 (n = 15)	LasCruces4 (n = 21)	1.77	0.18	0.55	0.67	0.41	0.41
Larvae	ElTerrero (n = 15)	LasCruces3 (n = 14)	**6.63**	**0.01**	**0.02**	4.45	0.03	0.10
	ElTerrero (n = 15)	LasCruces4 (n = 15)	**6.94**	**0.01**	**0.02**	1.87	0.17	0.26
	LasCruces3 (n = 14)	LasCruces4 (n = 15)	0.49	0.48	0.48	1.10	0.29	0.29

below the threshold for inclusion in the heatmap and differential abundance analysis (Additional file 2).

Unlike the internal microbial niche, no microbial taxa was predominant in larval cuticle surface microbiota across all three collection sites. However, some taxa showed notable patterns of abundance between locations (Fig. 5). These included the genus *Azoarcus,* which was detected at low to moderate frequencies in 13 of 15 pools of larvae from El Terrero, at low frequency in a single pool of larvae from Las Cruces 3, and was not detected at all in Las Cruces 4 (Fig. 4b and 6). Similarly, ASVs assigned to the genus *Spirosoma* were detected at moderate frequencies in all pools of larvae from Las Cruces 4, but only in a few pools from the other two locations. ASVs assigned to the genus *Paucibacter* were present at relatively higher abundance in larvae from both Las Cruces 3 and El Terrero compared to those from Las Cruces 4. Those assigned to the genus *Acidovorax* were predominant in larvae from Las Cruces 3 and Las Cruces 4 in contrast to El Terrero. ASVs assigned to *Microbacterium, Bdellovibrio* and *Pelomonas* were present at moderate frequencies in larvae from both Las Cruces 3 and Las Cruces 4 but were not detected in El Terrero (Fig. 5). Bacterial taxa that were unique to each collection site comprised < 8% of larval cuticle surface microbiota (Fig. 3b), and were below the threshold for inclusion in the heatmap and differential abundance analysis (Additional file 2).

Laboratory-colonized adult F1 *An. albimanus* were comprised of sparse internal and cuticle surface microbiota that were dominated by ASVs assigned to the genus Asaia

ASVs from adult internal microbiota were assigned to 62 microbial taxa and cuticle surface microbiota were assigned to 106 microbial taxa. Two of these ASVs which were only present in the cuticle surface microbiota were classified as archaea, while all other remaining ASVs were classified as bacteria (Additional file 2). Unlike larval microbiota, less than half of the assigned taxa across all locations (ranging from 19–37 taxa) were shared between internal and cuticle surface microbiota (Fig. 3a), and only 18 taxa on the cuticle surface and 19 internal taxa were shared across all maternal collection sites (Fig. 3b).

Overall, ASVs assigned to the bacterial genus *Asaia* dominated both adult internal and cuticle surface microbiota (Fig. 6), constituting at least 70% of taxa in each microbial niche (Additional file 2). A majority of identified taxa in adult internal, but not cuticle surface, microbiota was detected across all three collection sites, with a few of these taxa present in high abundance across all collection sites (Fig. 6). Across all three collection sites, ASVs assigned to the genera *Acinetobacter, Gluconobacter, Pantoea* and *Pseudomonas* were present in moderate to high abundance in adult internal microbiota in addition to *Asaia* (Fig. 6).

No site-specific microbial taxa were identified in adult cuticle surface microbiota, as the ASV distribution did not meet the criteria for this type of analysis. This was compounded by dominance (> 70%) of ASVs that were assigned to the bacterial genus *Asaia* (Additional file 2). In addition, the cuticle surface microbiota of adults originating from Las Cruces 4 comprised 43% of all adult cuticle surface microbial taxa (Fig. 3b), although a majority were of low abundance.

Discussion

The scientific community is increasingly investigating the role of mosquito microbiota in fighting mosquito-borne diseases [9]. The successful transition of mosquito microbiome research from laboratory to field requires a comprehensive understanding of the dynamics underlying the composition of the microbiota of field-collected

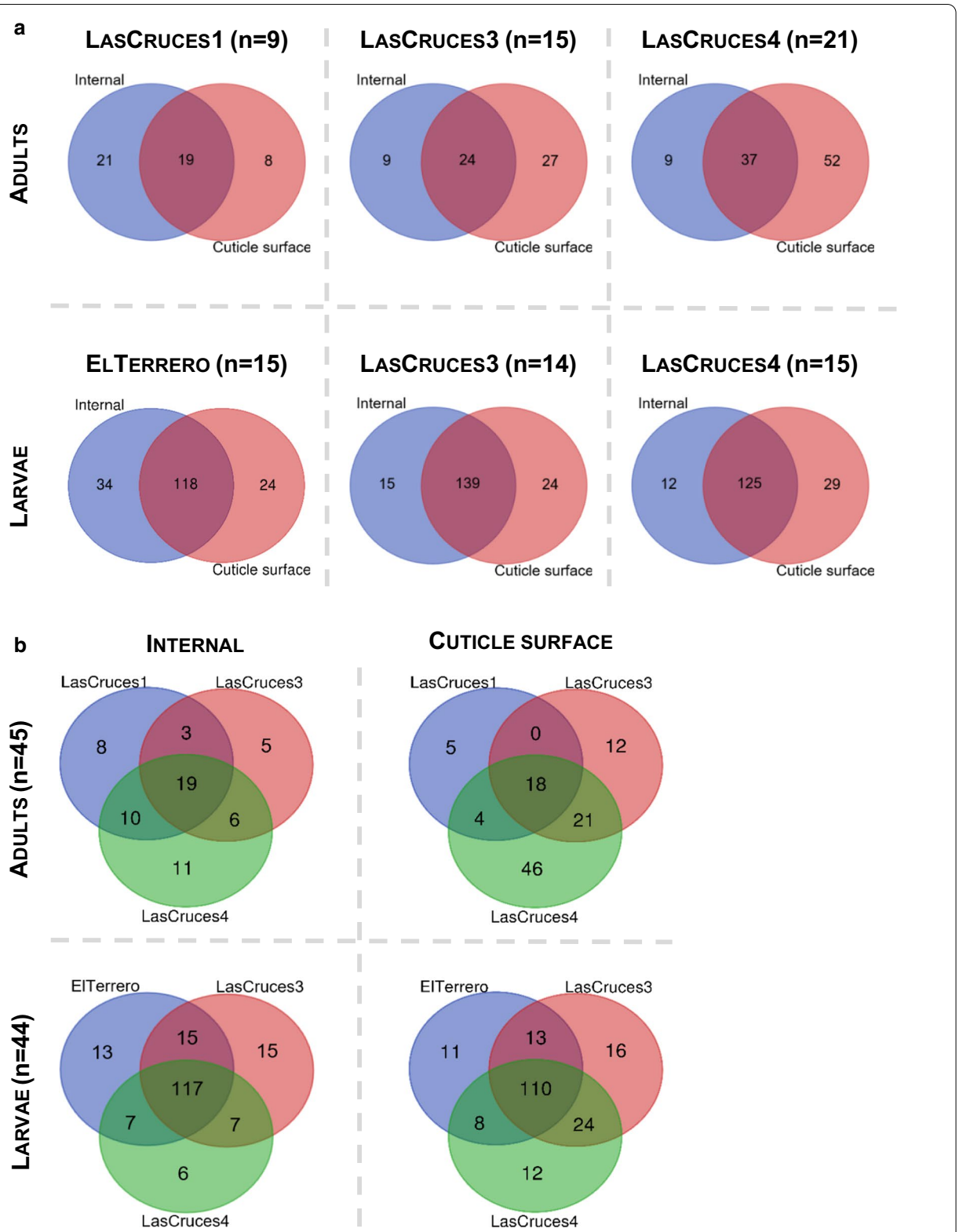

Fig. 3 Number of unique and shared microbial taxa between microbial niches (**A**) and number of unique and shared microbial taxa between collection sites (**B**). The number of taxa shown in the Venn diagram represent bacterial taxa except in the cuticle surface microbiota of adults from Las Cruces 4, where two archaeal taxa were present. n = pools of mosquito samples analyzed per location or microbial niche (3 individuals/pool)

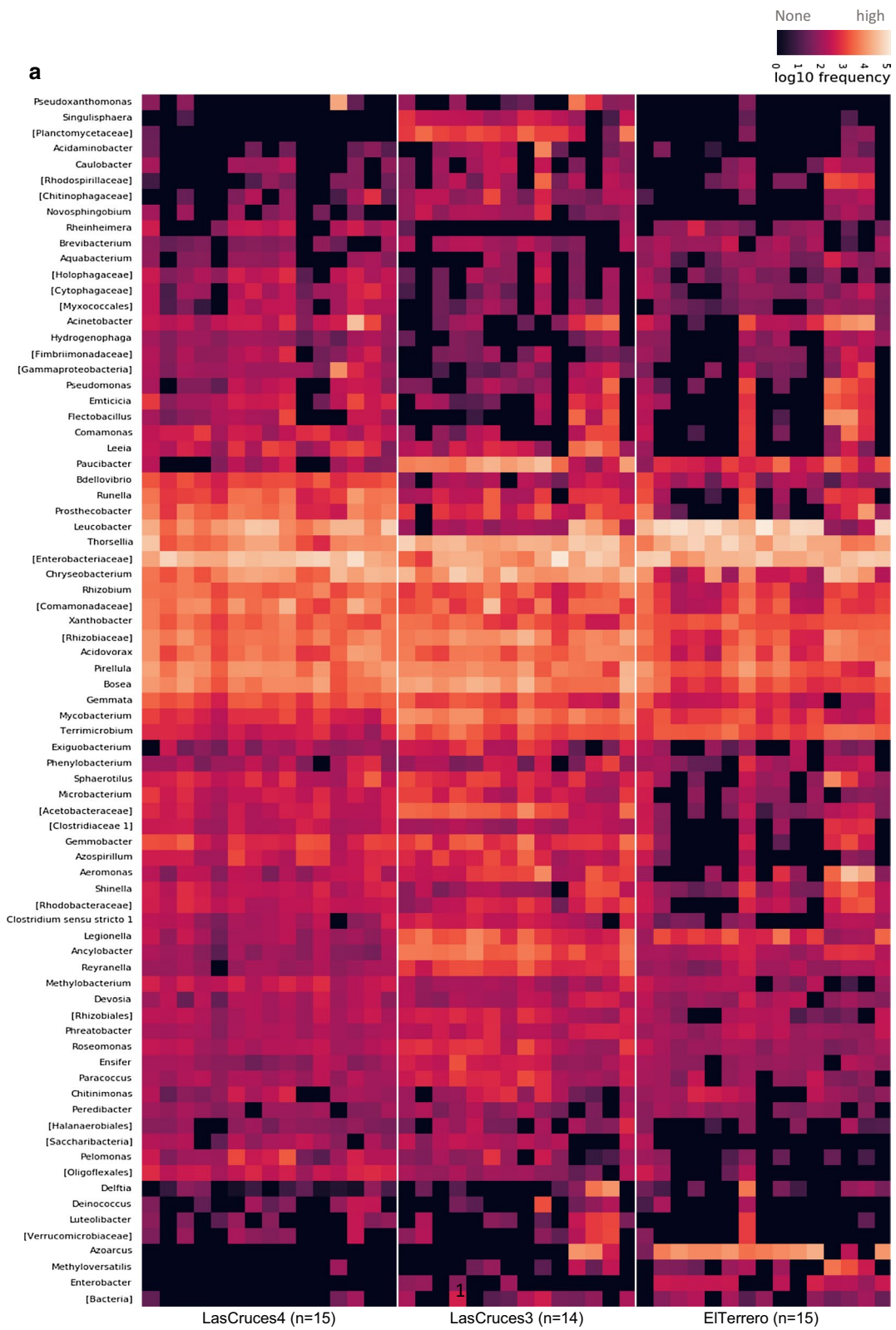

Fig. 4 Frequency of ASVs from the internal (**a**) and cuticle surface (**b**) microbiota of laboratory-colonized *An. albimanus* F_1 larvae originating from different collection sites. ASVs were annotated to the genus level or the lowest possible taxonomic level (in square brackets) and are clustered by the average nearest-neighbors chain algorithm. Only taxonomically annotated ASVs with frequencies ≥ 2000 are presented. n = pools of mosquito samples analyzed per location (3 individuals/pool)

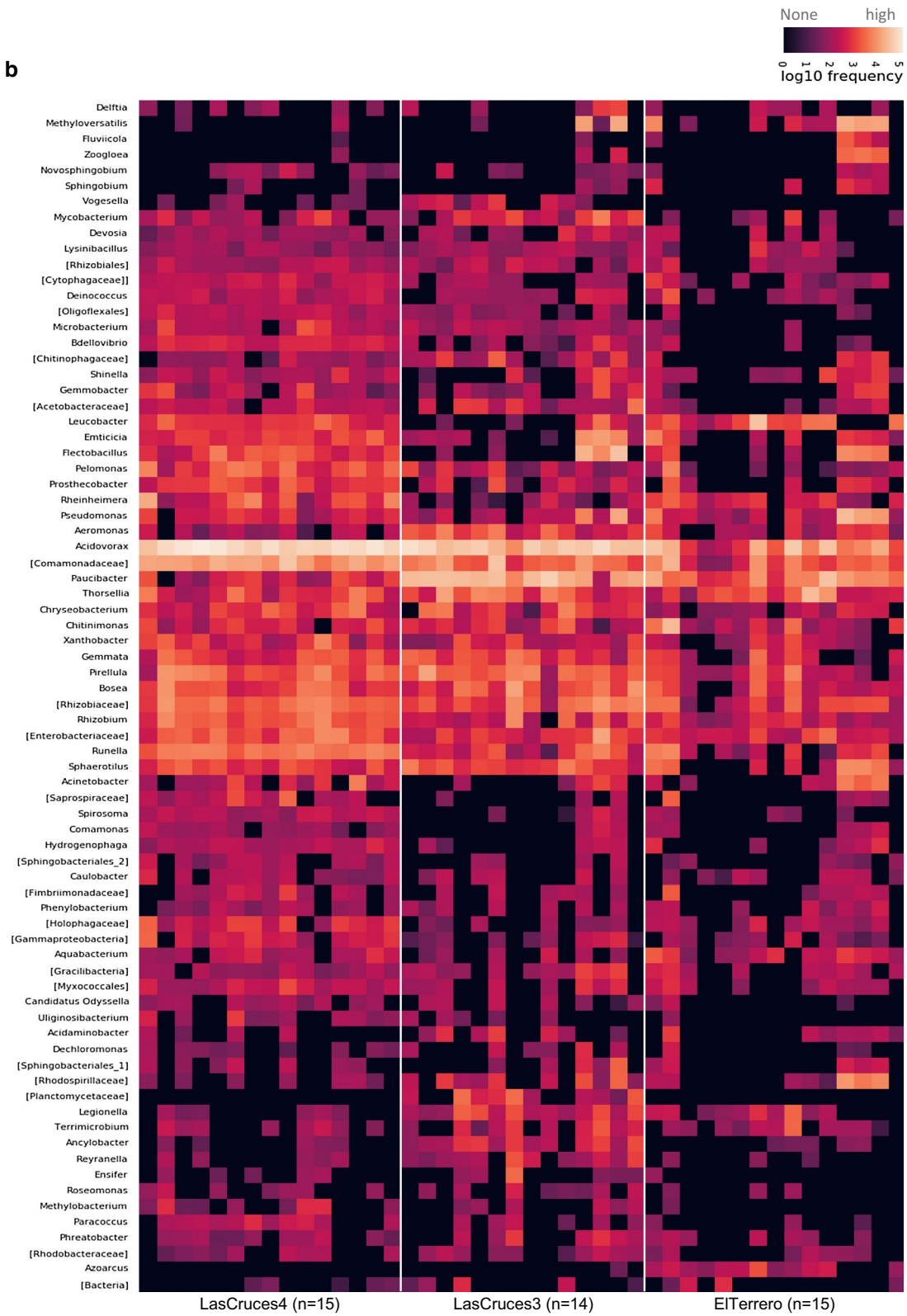

Fig. 4 continued

LARVAL INTERNAL MICROBIOTA

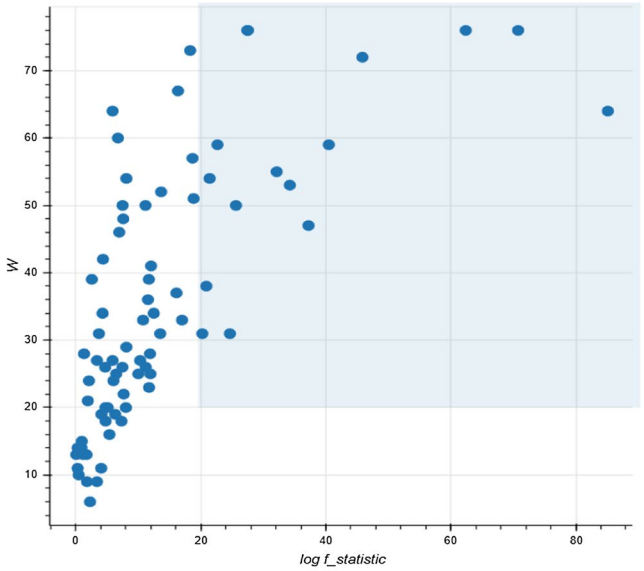

Significantly different taxa	W	ElTerrero	LasCruces3	LasCruces4
Singulisphaera	76		✓	
[Planctomycetaceae]	76		✓	
Paucibacter	76		✓	
Azoarcus	76	✓		
Azospirillum	72		✓	✓
Ancylobacter	64		✓	
Gemmobacter	59		✓	
Terrimicrobium	59	✓	✓	
Legionella	54	✓	✓	
[Oligoflexales]	55		✓	✓
Reyranella	53		✓	
[Acetobacteraceae]	50		✓	
Mycobacterium	47		✓	
[Saccharibacteria]	38		✓	✓
Bosea	31		✓	✓
Microbacterium	31		✓	✓

LARVAL CUTICLE SURFACE MICROBIOTA

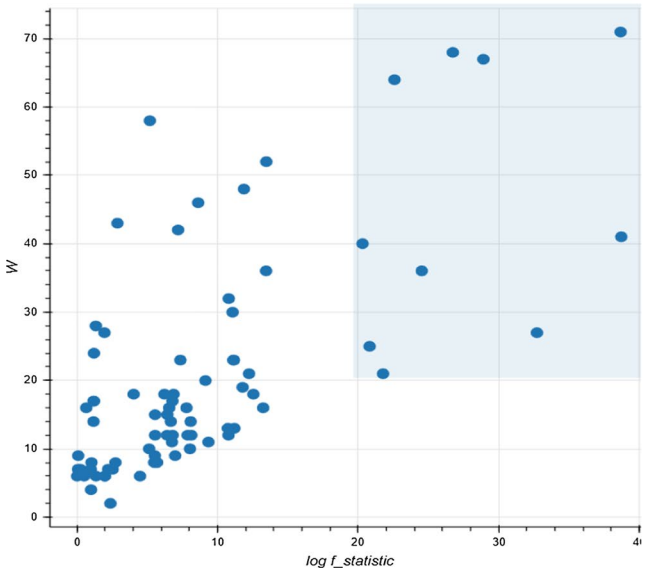

Significantly different taxa	W	ElTerrero	LasCruces3	LasCruces4
Azoarcus	71	✓		
Paucibacter	68	✓	✓	
[Planctomycetaceae]	67		✓	
Ancylobacter	64		✓	
Microbacterium	41		✓	✓
Spirosoma	40			✓
Bdellovibrio	36		✓	✓
[Oligoflexales]	27			✓
Pelomonas	25		✓	✓
Acidovorax	21		✓	✓

Fig. 5 Volcano plots of differentially abundant bacterial taxa in F_1 laboratory colonized *An. albimanus* larvae originating from three different collection sites. The plots show results of analysis of composition of microbiomes (ANCOM) tests for differentially abundant microbial taxa between collection site, with an effect size set to log F ≥ 20, and a cut-off of differential abundance set to W ≥ 20 (i.e., a taxon was differentially abundant across collection sites if the ratio of its abundance to those of at least 20 other taxa—25% of all included taxa—differed significantly across sites). Differentially abundant taxa are highlighted (blue shaded area), and the taxa names and locations in which they were most abundant are presented in the adjoining tables

mosquitoes and their progeny. Presented here is a comprehensive characterization of the internal and cuticle surface microbiota of laboratory-reared F_1 progeny from field-caught adult *An. albimanus* that were collected from different locations. Results show that while location-driven heterogeneity in the microbial community structure of both internal and cuticle surface microbiota was present in the F_1 larvae, this heterogeneity was only evident in the cuticle surface microbiota of adult progeny from the same generation. This work provides comprehensive fundamental data for studying how parentage

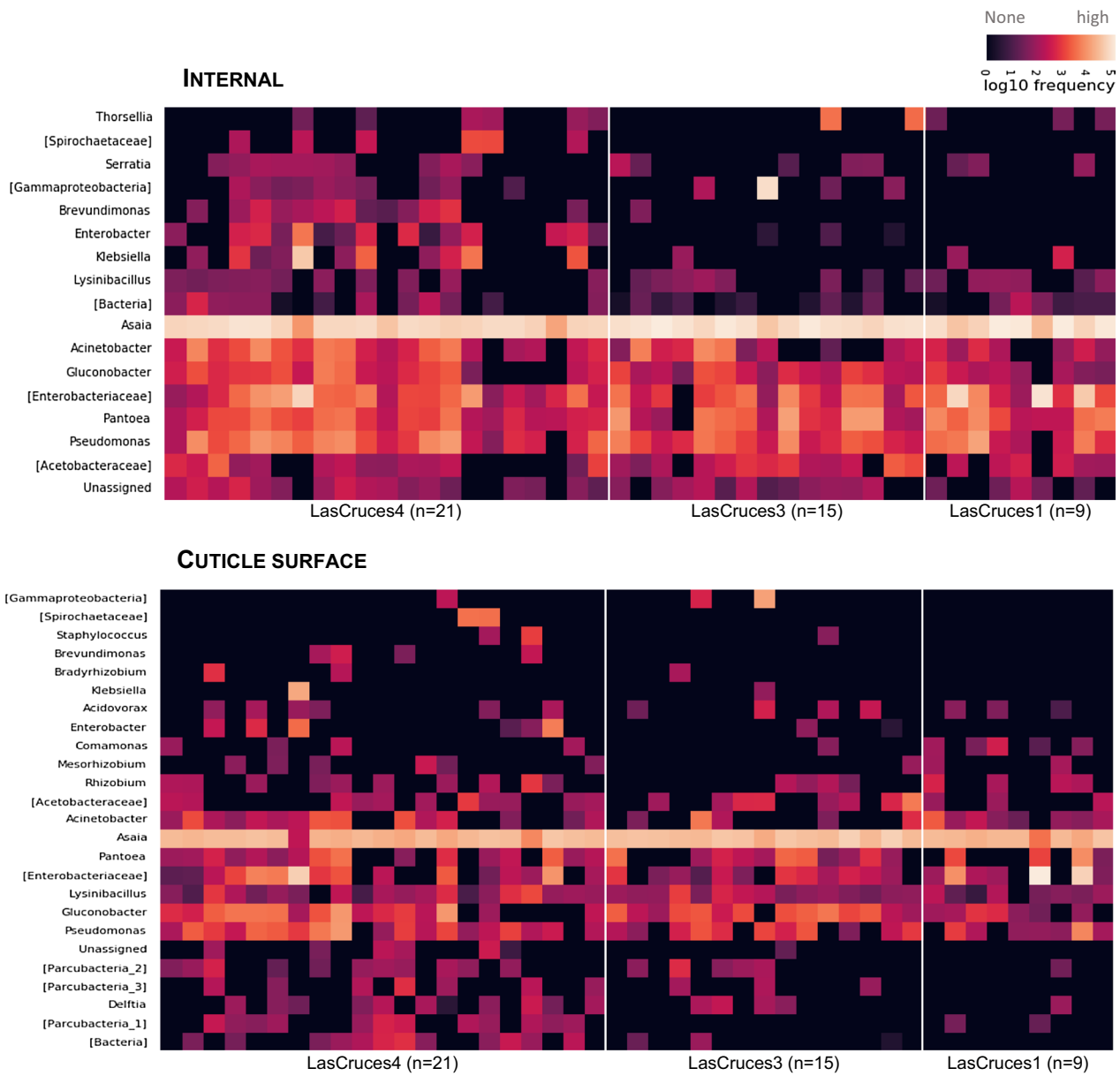

Fig. 6 Frequency of ASVs from the internal and cuticle surface microbiota of laboratory-colonized F_1 adult *An. albimanus* originating from different locations. ASVs were annotated to the genus level or the lowest possible taxonomic level (in square brackets) and are clustered by the average nearest-neighbors chain algorithm. Only taxonomically annotated ASVs with frequencies ≥ 1000 are presented. n = pools of mosquito samples analyzed per location (3 individuals/pool)

and environmental conditions differentially or concomitantly affect mosquito microbiome composition.

Previous studies on other mosquito species have also shown a loss of field-acquired internal mosquito microbiota following several generations of laboratory colonization [37, 38]. Until now, however, the laboratory generation at which this loss occurs was largely undescribed. This study represents an initial step in filling this knowledge gap and provides further details regarding the dynamics of changes in both the internal and cuticle surface microbial niches. The homogeneity in internal microbiota of F_1 adults is suggestive of a loss of field-acquired microbiota potentially due to laboratory rearing environment and sugar meal, which may have implications for studies that rely on laboratory progeny in lieu of field populations [25, 27, 28]. Previous findings

showed that rearing mosquitoes in water from the field could preserve the field-derived internal microbiota in laboratory-colonized adult progeny of *An. gambiae s.l.* for several generations [37]. In addition, other studies, have shown that the microbiota in larval habitat water significantly influences the internal microbiota of emerging adult mosquitoes [53, 54]. Thus, preserving wild-type microbiota in F_1 progeny could be an avenue for studying mosquito-microbe dynamics in the field.

Maternal egg-smearing has been proposed as a mechanism through which adult female mosquitoes and other insects transfer microbes to their progeny [55–58]. This transfer of microbes from mother to offspring via egg-smearing could explain the heterogeneity observed in internal and cuticle surface microbiota between F_1 larvae with different maternal origins. On the other hand, a lack of this heterogeneity in the internal microbiota of adult progeny could be attributed to a combination of (i) physiological changes that occur during metamorphosis and adult eclosion, whereby elimination of the larval meconial peritrophic membrane and meconium (midgut and midgut content), along with ingestion of exuvial fluid—which is said to be bactericidal—results in sterile or nearly sterile midguts in newly emerged adults [52, 59] and (ii) subsequent sugar meal and/or laboratory rearing environment. This could additionally be explained by mechanisms that regulate the composition of adult mosquito internal microbiota [60–62]. Conversely, the heterogeneity in cuticle surface microbiota between adult progeny originating from different maternal sites, suggests that maternally derived microbes in the rearing trays may have colonized adult cuticle surfaces during emergence. The mechanisms underlying the assemblage of the mosquito cuticle surface microbiome are largely undescribed, and thus require further investigation.

The low inter-sample variation in microbial diversity observed in this study has largely been described in other laboratory mosquito colonies [38, 63]. The microbial composition of laboratory-reared larvae is typically less diverse [63, 64] compared to those of field-derived larvae, but the laboratory-reared larvae in the current study exhibited a rich microbial composition that was comparable to those of previously studied field populations [52, 53]. In contrast, the adult progeny in the current study had a less diverse microbial composition that was reflective of typical laboratory-reared adult mosquitoes [36, 65]. This further suggests that field-acquired microbiota, although transferred to laboratory progeny, may be lost within one generation of laboratory colonization—particularly at the adult stage.

In this study, microbial taxa that have previously been identified in *Anopheles* and other mosquito genera [7, 18, 54, 66] were detected. While a majority of the taxa in F_1 larvae were shared between both the internal and cuticle surface microbial niches, a greater abundance of microbial taxa was detected in the internal microbial niche compared to the cuticle surface. The cuticle surface microbiota of mosquitoes and other haematophagous insects are largely uncharacterized and the mechanisms underlying their assemblage remain unknown. As such, we hypothesize that although both internal and cuticle surface niches are exposed to the same water from which the microbiota is derived, a more conducive and/or selective internal environment could allow for greater proliferation of colonizing bacteria. In F_1 adults however, less than half of the detected microbial taxa were shared between the internal and cuticle surface microbial niches, suggesting differences in physiological conditions that favor microbial colonization, and corroborating findings that point toward microbial regulatory mechanisms within the mosquito midgut [60–62]. Although a few microbial taxa overlapped between adult internal and cuticle surface microbial niches and the most abundant taxa were shared, many of the unshared taxa have been previously detected in adult mosquitoes including *Anopheles* [1, 18, 67], indicating that the cuticle surface microbiota characterized in this study are inherently associated with mosquitoes. Like the larval microbiota, there was a higher abundance of microbial taxa in the adult internal microbial niche compared to the cuticle surface, further supporting the hypothesis of a more conducive and/or selective internal environment. Potential loss of some microbes during sample storage is also plausible.

With the exception of the adult cuticle surface microbial niche, a majority of all detected microbial taxa overlapped between collection sites in both F_1 larvae and adults, albeit with differing abundances. This may effects of controlled laboratory environments on the development of mosquito microbiota. In the internal and cuticle surface of larvae and adult samples, microbial taxa that were specific to collection sites were low in abundance, compared to the moderate to high abundance of those that were shared across all locations. This was particularly true for *Asaia*—notorius for rapidly colonizing laboratory mosquitoes [68]—which constituted at least 70% of both adult internal and cuticle surface microbiota from progeny across all collection sites. These results suggest that field-acquired mosquito microbiota may be lost in as early as the first generation of laboratory colonization.

Conclusion

A limitation of this study is the lack of microbial community profiles of the mothers and the larval habitats from which the F_1 progeny were derived. However, the findings

herein provide empirical data on the composition of laboratory reared F_1 *An. albimanus* microbiota from different locations. It provides a foundation for exploring the role of parentage, environmental conditions, and inherent host physiological characteristics on the assemblage of the mosquito microbiome, as well as the fate of field-derived microbes upon laboratory colonization. This is critical for advancing mosquito microbiome studies and their applications beyond laboratory settings.

Supplementary Information

The online version contains supplementary material available at https://doi.org/10.1186/s12936-021-03934-5.

Additional file 1. Shannon alpha diversity plots.

Additional file 2. Frequency and relative abundance of microbial taxa detected in internal and cuticle surface microbiota of F1 laboratory colonized *An. albimanus* larvae and adults.

Additional file 3. Summary statistics of sequencing reads and amplicon sequence variants (ASVs) used for downstream analysis.

Additional file 4. Rarefaction depth and plots of sequencing reads.

Additional file 5. Results of downstream analysis including low frequency (potentially extraneous) reads.

Acknowledgements
We thank the cattle coral owners in Escuintla, Guatemala for permission to conduct mosquito collections within their corals, without which this study would not have been possible; the Malaria Research and Reference Reagent Resource Center (MR4) for providing the ITS2 primers and *Anopheles albimanus* DNA used for *An. albimanus* species identification; Nelson Jimenez and Ricardo Santos from the Ministerio de Salud Publica y Asistencia Social (MSPAS) for assistance during mosquito collections; and Daniela Da'Costa, Pedro Peralta, Adel Mejia and Alfonso Salam from Universidad del Valle de Guatemala (UVG) for field support and assistance during mosquito rearing. The adult mosquito icon used in Fig. 1 was created by MarkieAnn Packer from the Noun Project. The findings and conclusions in this paper are those of the authors and do not necessarily represent the official position of the US Centers for Disease Control and Prevention (CDC) or the American Society for Microbiology (ASM).

Authors' contributions
ND† & AL conceptualized and designed the study; NP facilitated and provided facilities for field work; ND†, ACB, FL & JCL performed mosquito collections, and mass rearing; ND† & MS performed molecular analysis and sequencing; ND† analysed the data; ND† and ND performed the data visualizations; ND† drafted the manuscript. All authors read and approved the final manuscript.

Funding
This work was supported by the US Centers for Disease Control and Prevention (CDC) through the American Society for Microbiology's (ASM) Infectious Disease and Public Health Microbiology Postdoctoral Fellowship awarded to ND†, and the CDC's Advanced Molecular Detection (AMD) program.

Availability of data and material
The raw sequencing reads generated from this project, including those from negative controls (blanks), have been deposited in the National Center for Biotechnology Information (NCBI), Sequence Read Archive under the BioProject PRJNA512122.

Declarations

Ethics approval and consent to participate
Not applicable.

Consent for publication
Not applicable.

Competing interests
The authors declare that they have no competing interests.

Author details
[1]Entomology Branch, Division of Parasitic Diseases and Malaria, Center for Global Health, United States Centers for Diseases Control and Prevention, Atlanta, GA, USA. [2]Grupo de Biología Y Control de Vectores, Centro de Estudios en Salud, Universidad del Valle de Guatemala, Guatemala City, Guatemala. [3]Biotechnology Core Facility Branch, Division of Scientific Resources, National Center for Emerging & Zoonotic Infectious Diseases, United States Centers for Disease Control and Prevention, Atlanta, GA, USA. [4]American Society for Microbiology, Washington, DC, USA. [5]Tropical Infectious Diseases Research Center, University of Abomey-Calavi, Cotonou, Benin.

Received: 19 May 2021 Accepted: 30 September 2021
Published online: 23 October 2021

References

1. Guégan M, Zouache K, Démichel C, Minard G, Van Tran V, Potier P, et al. The mosquito holobiont: fresh insight into mosquito-microbiota interactions. Microbiome. 2018;6:49.
2. Coon KL, Brown MR, Strand MR. Mosquitoes host communities of bacteria that are essential for development but vary greatly between local habitats. Mol Ecol. 2016;25:5806–26.
3. Lindh JM, Borg-Karlson AK, Faye I. Transstadial and horizontal transfer of bacteria within a colony of *Anopheles gambiae* (Diptera: Culicidae) and oviposition response to bacteria-containing water. Acta Trop. 2008;107:242–50.
4. Dickson LB, Jiolle D, Minard G, Moltini-Conclois I, Volant S, Ghozlane A, et al. Carryover effects of larval exposure to different environmental bacteria drive adult trait variation in a mosquito vector. Sci Adv. 2017;3:e1700585–e1700585.
5. Dennison NJ, Jupatanakul N, Dimopoulos G. The mosquito microbiota influences vector competence for human pathogens. Curr Opin Insect Sci. 2014;3:6–13.
6. Coon KL, Brown MR, Strand MR. Gut bacteria differentially affect egg production in the anautogenous mosquito *Aedes aegypti* and facultatively autogenous mosquito *Aedes atropalpus* (Diptera: Culicidae). Parasit Vectors. 2016;9:375.
7. Dada N, Sheth M, Liebman K, Pinto J, Lenhart A. Whole metagenome sequencing reveals links between mosquito microbiota and insecticide resistance in malaria vectors. Sci Rep. 2018;8:2084.
8. Dada N, Lol JC, Benedict AC, López F, Sheth M, Dzuris N, et al. Pyrethroid exposure alters internal and cuticle surface bacterial communities in *Anopheles albimanus*. ISME J. 2019;13:2447–64.
9. Huang W, Wang S, Jacobs-Lorena M. Use of microbiota to fight mosquito-borne disease. Front Genet. 2020;11:196.
10. Luis P, Vallon L, Tran F-H, Hugoni M, Tran-Van V, Mavingui P, et al. *Aedes albopictus* mosquitoes host a locally structured mycobiota with evidence of reduced fungal diversity in invasive populations. Fungal Ecol. 2019;39:257–66.
11. Thongsripong P, Chandler JA, Green AB, Kittayapong P, Wilcox BA, Kapan DD, et al. Mosquito vector-associated microbiota: metabarcoding bacteria and eukaryotic symbionts across habitat types in Thailand endemic for dengue and other arthropod-borne diseases. Ecol Evol. 2018;8:1352–68.
12. Shi C, Beller L, Deboutte W, Yinda KC, Delang L, Vega-Rúa A, et al. Stable distinct core eukaryotic viromes in different mosquito species from Guadeloupe, using single mosquito viral metagenomics. Microbiome. 2019;7:121.
13. Atoni E, Wang Y, Karungu S, Waruhiu C, Zohaib A, Obanda V, et al. Metagenomic virome analysis of *Culex* mosquitoes from Kenya and China. Viruses. 2018;10:30.
14. Crawford JE, Clarke DW, Criswell V, Desnoyer M, Cornel D, Deegan B, et al. Efficient production of male Wolbachia-infected *Aedes aegypti* mosquitoes enables large-scale suppression of wild populations. Nat Biotechnol. 2020;38:482–92.

15. Flores HA, de Bruyne J, Donnell TB, Tuyet Nhu V, Thi Giang N, Trang H, et al. Multiple *Wolbachia* strains provide comparative levels of protection against dengue virus infection in *Aedes aegypti*. PLoS Pathog. 2020;16:e1008433.
16. Capone A, Ricci I, Damiani C, Mosca M, Rossi P, Scuppa P, et al. Interactions between *Asaia*, *Plasmodium* and *Anopheles*: new insights into mosquito symbiosis and implications in Malaria Symbiotic Control. Parasit Vectors. 2013;6:182.
17. Wang S, Dos-Santos ALA, Huang W, Liu KC, Oshaghi MA, Wei G, et al. Driving mosquito refractoriness to *Plasmodium falciparum* with engineered symbiotic bacteria. Science. 2017;357:1399–402.
18. Villegas LM, Pimenta PF. Metagenomics, paratransgenesis and the *Anopheles* microbiome: a portrait of the geographical distribution of the anopheline microbiota based on a meta-analysis of reported taxa. Mem Inst Oswaldo Cruz. 2014;109:672–84.
19. Bascuñán P, Niño-Garcia JP, Galeano-Castañeda Y, Serre D, Correa MM. Factors shaping the gut bacterial community assembly in two main Colombian malaria vectors. Microbiome. 2018;6:148.
20. Galeano-Castañeda Y, Urrea-Aguirre P, Piedrahita S, Bascuñán P, Correa MM. Composition and structure of the culturable gut bacterial communities in *Anopheles albimanus* from Colombia. PLoS One. 2019;14:e0225833.
21. Prussing C, Saavedra MP, Bickersmith SA, Alava F, Guzmán M, Manrique E, et al. Malaria vector species in Amazonian Peru co-occur in larval habitats but have distinct larval microbial communities. PLoS Negl Trop Dis. 2019;13:e0007412.
22. Hiwat H, Bretas G. Ecology of *Anopheles darlingi* Root with respect to vector importance: a review. Parasit Vectors. 2011;4:177.
23. Villarreal-Treviño C, Penilla-Navarro RP, Vázquez-Martínez MG, Moo-Llanes DA, Ríos-Delgado JC, Fernández-Salas I, et al. Larval habitat characterization of *Anopheles darlingi* from its northernmost geographical distribution in Chiapas. Mexico Malar J. 2015;14:517.
24. Fillinger U, Sombroek H, Majambere S, van Loon E, Takken W, Lindsay SW. Identifying the most productive breeding sites for malaria mosquitoes in The Gambia. Malar J. 2009;8:62.
25. Gimnig JE, Ombok M, Kamau L, Hawley WA. Characteristics of larval anopheline (*Diptera: Culicidae*) habitats in Western Kenya. J Med Entomol. 2001;38:1.
26. Greico JP, Johnson S, Achee NL, Masuoka P, Pope K, Rejmánková E, et al. Distribution of *Anopheles albimanus*, *Anopheles vestitipennis*, and *Anopheles crucians* Associated with Land Use in Northern Belize. J Med Entomol. 2006;43:614–22.
27. Tchigossou G, Akoton R, Yessoufou A, Djegbe I, Zeukeng F, Atoyebi SM, et al. Water source most suitable for rearing a sensitive malaria vector, *Anopheles funestus* in the laboratory. Wellcome Open Res. 2017;2:109.
28. Benedict MQ, Knols BGJ, Bossin HC, Howell PI, Mialhe E, Caceres C, et al. Colonisation and mass rearing: learning from others. Malar J. 2009;8:S4.
29. World Health Organization. Anopheline species complexes in south-east Asia. WHO Regional Office for South-East Asia; 1998.
30. Rosa-Freitas MG, Lourenço-de-Oliveira R, de Carvalho-Pinto CJ, Flores-Mendoza C, Silva-do-Nascimento TF. Anopheline species complexes in Brazil. Current knowledge of those related to malaria transmission. Mem Inst Oswaldo Cruz. 1998;93:651–5.
31. Cohuet A, Simard F, Toto JC, Kengne P, Coetzee M, Fontenille D. Species identification within the *Anopheles funestus* group of malaria vectors in Cameroon and evidence for a new species. Am J Trop Med Hyg. 2003;69:200–5.
32. Stevenson JC, Norris DE. Implicating cryptic and novel anophelines as malaria vectors in Africa. Insects. 2016;8:1.
33. Omoke D, Kipsum M, Otieno S, Esalimba E, Sheth M, Lenhart A, et al. Western Kenyan *Anopheles gambiae* showing intense permethrin resistance harbour distinct microbiota. Malar J. 2021;20:77.
34. Duguma D, Hall MW, Smartt CT, Debboun M, Neufeld JD. Microbiota variations in *Culex nigripalpus* disease vector mosquito of West Nile virus and Saint Louis Encephalitis from different geographic origins. Peer J. 2019;6:e6168.
35. Muturi EJ, Lagos-Kutz D, Dunlap C, Ramirez JL, Rooney AP, Hartman GL, et al. Mosquito microbiota cluster by host sampling location. Parasit Vectors. 2018;11:468.
36. Coon KL, Vogel KJ, Brown MR, Strand MR. Mosquitoes rely on their gut microbiota for development. Mol Ecol. 2014;23:2727–39.
37. Akorli J, Namaali PA, Ametsi GW, Egyirifa RK, Pels NAP. Generational conservation of composition and diversity of field-acquired midgut microbiota in *Anopheles gambiae* (sensu lato) during colonization in the laboratory. Parasit Vectors. 2019;12:27.
38. Dickson LB, Ghozlane A, Volant S, Bouchier C, Ma L, Vega-Rua A, et al. Diverse laboratory colonies of *Aedes aegypti* harbor the same adult midgut bacterial microbiome. Parasit Vectors. 2018;11:207.
39. Wilkerson RC, Strickman D, Litwak TR. Illustrated key to the female anopheline mosquitoes of Central America and Mexico. J Am Mosq Control Assoc. 1990;6:7–34.
40. Wej Choochote, Atiporn Saeung. Systematic techniques for the recognition of *Anopheles* species complexes. In: Manguin S, Ed. *Anopheles* mosquitoes. IntechOpen; 2013.
41. Beebe NW, Saul A. Discrimination of all members of the Anopheles punctulatus complex by polymerase chain reaction–restriction fragment length polymorphism analysis. Am J Trop Med Hyg. 1995;53:478–81.
42. MR4. Amplification of the second internal transcribed spacer region (ITS2) in *Anophelines*. Methods in *Anopheles* research. BEI Resources; 2015.
43. Bolyen E, Rideout JR, Dillon MR, Bokulich NA, Abnet CC, Al-Ghalith GA, et al. Reproducible, interactive, scalable and extensible microbiome data science using QIIME 2. Nat Biotechnol. 2019;37:852–7.
44. Callahan BJ, McMurdie PJ, Rosen MJ, Han AW, Johnson AJA, Holmes SP. DADA2: High-resolution sample inference from Illumina amplicon data. Nat Methods. 2016;13:581.
45. Crawley MJ. The R book. New York: John Wiley & Sons; 2012.
46. McMurdie PJ, Holmes S. phyloseq: An R package for reproducible interactive analysis and graphics of microbiome census data. PLoS One. 2013;8:e61217.
47. Harry Zhang. The optimality of Naive Bayes. 2004.
48. Bokulich NA, Kaehler BD, Rideout JR, Dillon M, Bolyen E, Knight R, et al. Optimizing taxonomic classification of marker-gene amplicon sequences with QIIME 2's q2-feature-classifier plugin. Microbiome. 2018;6:90.
49. Quast C, Pruesse E, Yilmaz P, Gerken J, Schweer T, Yarza P, et al. The SILVA ribosomal RNA gene database project: improved data processing and web-based tools. Nucleic Acids Res. 2013;41:D590–6.
50. Mandal S, Van Treuren W, White RA, Eggesbo M, Knight R, Peddada SD. Analysis of composition of microbiomes: a novel method for studying microbial composition. Microb Ecol in Health Dis. 2015;26:27663.
51. Inkscape team. Inkscape: http://www.inkscape.org/. 2004.
52. Duguma D, Hall MW, Rugman-Jones P, Stouthamer R, Terenius O, Neufeld JD, et al. Developmental succession of the microbiome of *Culex* mosquitoes. BMC Microbiol. 2015;15:140.
53. Gimonneau G, Tchioffo MT, Abate L, Boissière A, Awono-Ambéné PH, Nsango SE, et al. Composition of *Anopheles coluzzii* and *Anopheles gambiae* microbiota from larval to adult stages. Infect Genet Evol. 2014;28:715–24.
54. Saab SA, Dohna H, Nilsson LKJ, Onorati P, Nakhleh J, Terenius O, et al. The environment and species affect gut bacteria composition in laboratory co-cultured *Anopheles gambiae* and *Aedes albopictus* mosquitoes. Sci Rep. 2020;10:3352.
55. Damiani C, Ricci I, Crotti E, Rossi P, Rizzi A, Scuppa P, et al. Mosquito-bacteria symbiosis: the case of *Anopheles gambiae* and *Asaia*. Microb Ecol. 2010;60:644–54.
56. Rossi P, Ricci I, Cappelli A, Damiani C, Ulissi U, Mancini MV, et al. Mutual exclusion of *Asaia* and *Wolbachia* in the reproductive organs of mosquito vectors. Parasit Vectors. 2015;8:278.
57. Benedict MQ. Transgenic insects: techniques and applications. CABI; 2014.
58. Crotti E, Rizzi A, Chouaia B, Ricci I, Favia G, Alma A, et al. Acetic acid bacteria, newly emerging symbionts of insects. Appl Environ Microbiol. 2010;76:1.
59. Moll RM, Romoser WS, Modrzakowski MC, Moncayo AC, Lerdthusnee K. Meconial peritrophic membranes and the fate of midgut bacteria during mosquito (*Diptera: Culicidae*) metamorphosis. J Med Entomol. 2001;38:29–32.
60. Rodgers FH, Gendrin M, Wyer CAS, Christophides GK. Microbiota-induced peritrophic matrix regulates midgut homeostasis and prevents systemic infection of malaria vector mosquitoes. PLoS Pathog. 2017;13:e1006391.
61. Song X, Wang M, Dong L, Zhu H, Wang J. PGRP-LD mediates A stephensi vector competency by regulating homeostasis of microbiota-induced peritrophic matrix synthesis. PLoS Pathog. 2018;14:e1006899.

62. Gao L, Song X, Wang J. Gut microbiota is essential in PGRP-LA regulated immune protection against *Plasmodium berghei* infection. Parasit Vectors. 2020;13:3–3.
63. Minard G, Tran F-H, Van Tran V, Fournier C, Potier P, Roiz D, et al. Shared larval rearing environment, sex, female size and genetic diversity shape *Ae. albopictus* bacterial microbiota. PLoS One. 2018;13:e0194521.
64. Short SM, Mongodin EF, MacLeod HJ, Talyuli OAC, Dimopoulos G. Amino acid metabolic signaling influences *Aedes aegypti* midgut microbiome variability. PLOS Negl Trop Dis. 2017;11:e0005677.
65. Boissière A, Tchioffo MT, Bachar D, Abate L, Marie A, Nsango SE, et al. Midgut microbiota of the malaria mosquito vector *Anopheles gambiae* and interactions with *Plasmodium falciparum* infection. PLoS Pathog. 2012;8:e1002742–e1002742.
66. Hegde S, Khanipov K, Albayrak L, Golovko G, Pimenova M, Saldaña MA, et al. Microbiome interaction networks and community structure from laboratory-reared and field-collected *Aedes aegypti*, *Aedes albopictus*, and *Culex quinquefasciatus* mosquito vectors. Front Microbiol. 2018;9:2160–2160.
67. Dinparast Djadid N, Jazayeri H, Raz A, Favia G, Ricci I, Zakeri S. Identification of the midgut microbiota of *An. stephensi* and *An. maculipennis* for their application as a paratransgenic tool against malaria. PLoS One. 2011;6:e28484.
68. Favia G, Ricci I, Damiani C, Raddadi N, Crotti E, Marzorati M, et al. Bacteria of the genus *Asaia* stably associate with *Anopheles stephensi*, an Asian malarial mosquito vector. Proc Natl Acad Sci USA. 2007;104:9047–51.

Publisher's Note